Confined micro-environment of micelles regulates their interaction with anions

Pan Sun,[ab]* Wei Bu,[b] Binhua Lin,[b] Mark L. Schlossman,[a] and Mrinal K. Bera[b]*

a. Department of Physics, University of Illinois at Chicago, Chicago, IL 60607, USA

b. NSF's ChemMatCARS, University of Chicago, Chicago, IL 60637, USA

Abstract: Ion interactions with supramolecular assemblies underlie their applications in the areas of drug delivery, ion recognition, and conduction. The current challenge remains in directly characterizing the interaction of ions with supramolecular assemblies at the nanoscale. Here, we demonstrate that the micro-environment of neutral polymer micelles regulates its interaction with anions by combining element-sensitive anomalous small angle X-ray scattering (ASAXS) and theoretical calculations. ASAXS and molecular dynamics simulations reveal that monovalent ReO_4^- is located preferentially in the outer shell of the micelle, while the more strongly hydrated divalent SeO_4^{2-} is excluded from the micelle. However, DFT calculations show that the more highly charged SeO_4^{2-} should have stronger affinity for an isolated polymer chain than ReO_4^-. These results suggest that the confined environment created by polymer self-assembly modulates the contribution of hydrophobic and electrostatic interactions to the binding of anions with polymers. The present work sheds light on the role of crowded environments in the interaction of anions with polymers in supramolecular assemblies and offers valuable insights to optimize the design of supramolecular systems.

Block copolymers containing immiscible blocks can self-assemble into highly ordered multimolecular architectures, including micelles and vesicles.[1-7] These architectures have been investigated for their ability to provide a tunable environment for nano-materials synthesis, drug delivery, and ion recognition and conduction.[8-10] It is well known that ions influence the self-assembly of amphiphilic block copolymers, regulating the interaction of block copolymers with their surroundings.[11-13] Nevertheless, the molecular-level mechanisms that underlie the effect of ions on these systems remain unclear. An improved fundamental understanding of ion interactions with self-assembled block copolymers should contribute to advancing their applications.

Interactions of ions with block co-polymers are highly dependent on the specific characteristics of both the ion and the polymer block. For example, charged polymer blocks such as polyelectrolytes interact strongly with oppositely charged ions through electrostatic forces.[14-15] While the interactions of anions with neutral polymers are not as well understood, these interactions are often divided into two categories: direct and indirect.[16] Direct interactions involve anions shedding their hydration shells and subsequent hydrophobic interactions with the polymer.[17-18] Hydrophobic interactions occur between nonpolar or weakly polar molecules in the presence of water, as the water molecules preferentially interact with each other rather than with the nonpolar molecules. The anion can thus adsorb onto the polymer through hydrophobic interactions, which can be facilitated by the shedding of the ion's hydration shell.[19] Indirect interactions consist of the electrostatic attraction of anions to cations that have coordinated with oxygen sites on the polymer.[20-22] This electrostatic interaction can also be facilitated by the hydration behavior of the anion. In both direct and indirect interactions, the hydration behavior of the anion is crucial in breaking the hydrogen-bond network around the polymer and overcoming the hydration barrier between the anion and polymer.[23-24] Related to this is a recent suggestion that the local curvature of a polymer chain plays a role in their affinity to anions.[23] Anion-polymer interaction mechanisms and the role of hydration have been explored by SFG,[25-27] electrophoretic NMR,[28-29] and tensiometry.[30-31] Notably, these interaction of polymer with anions were usually measured indirectly from the environmental change[25, 29] of the polymer chain that may be induced by the anion binding, directly measurement of anion binding to the polymer is still challenging.

The interaction of anions with polymers in real application processes can be more complex due to the self-assembly of polymers in water.[32] The crowded environment of a polymer within an assembled structure is significantly different from the environment before aggregation and may

include more disordered water, reduced chain flexibility, and strong polymer-polymer interactions.[33-34] The environment created by copolymer assembly makes it challenging to study anion-polymer interactions.

Here, we use anomalous small angle X-ray scattering (ASAXS) to directly measure anion distributions near and within self-assembled co-polymer micelles. These distributions provide direct evidence of the interactions of anions within complex polymer architectures.[20, 35] ASAXS is a powerful technique for analyzing the spatial distribution of a target element in nano-scale particles.[36-37] ASAXS probes this distribution by measuring the energy dependence of small-angle X-ray scattering near the absorption edge of a targeted element. The success of this technique relies upon targeting elements whose absorption edge energies are accessible by the chosen x-ray source, as well as on the use of particles with narrow size and shape distributions.

Our ASAXS measurements probe micelles self-assembled from the linear triblock copolymer Pluronic P123 and two anions, SeO_4^{2-} and ReO_4^{-}, whose different hydration behavior[38] allows us to investigate the role of hydration in anion-polymer interactions. P123 consists of a 70-monomer block of poly(propylene oxide) (PPO) sandwiched between two 20-monomer blocks of poly(ethylene oxide) (PEO), as shown in Figure 1D. It forms a well-defined spherical micelle in water and SeO_4^{2-} and ReO_4^{-} have accessible x-ray absorption edge energies, which make this system suitable for study by ASAXS. Additionally, molecular dynamics (MD) simulations and density functional theory (DFT) calculations contribute to a molecular-level understanding of the ion distributions within P123 micelles.

ASAXS simulations of anion distributions in the micelle

ASAXS is a measurement of small angle X-ray scattering using X-rays with energies near the electronic absorption energy of the target element for the purpose of measuring the spatial distribution of that element. Figures 1A and 1B show examples of ASAXS measurements from aqueous solutions of P123 (5% weight fraction, P123 illustrated in Fig. 1D) containing either 5 mM NaReO$_4$ or 5 mM Na$_2$SeO$_4$, respectively, at three different energies near absorption edges of Re (Lα3 edge, 10.52 keV) and Se (K edge, 12.65 keV). Lines show fits to the different energy data sets, which are nearly identical for SeO_4^{2-} but differ for ReO_4^{-}. The fits were obtained using XModFit,[39] the software developed at NSF's ChemMatCARS for modeling and fitting X-ray scattering data. Figure 1C shows that the scattering intensity at a fixed value of wave vector

4

transfer Q varies substantially with energy near the Lα3 absorption edge of Re for samples containing ReO_4^-, whereas the intensity is relatively insensitive to the variation in X-ray energy near the K edge of Se for samples containing SeO_4^{2-}.
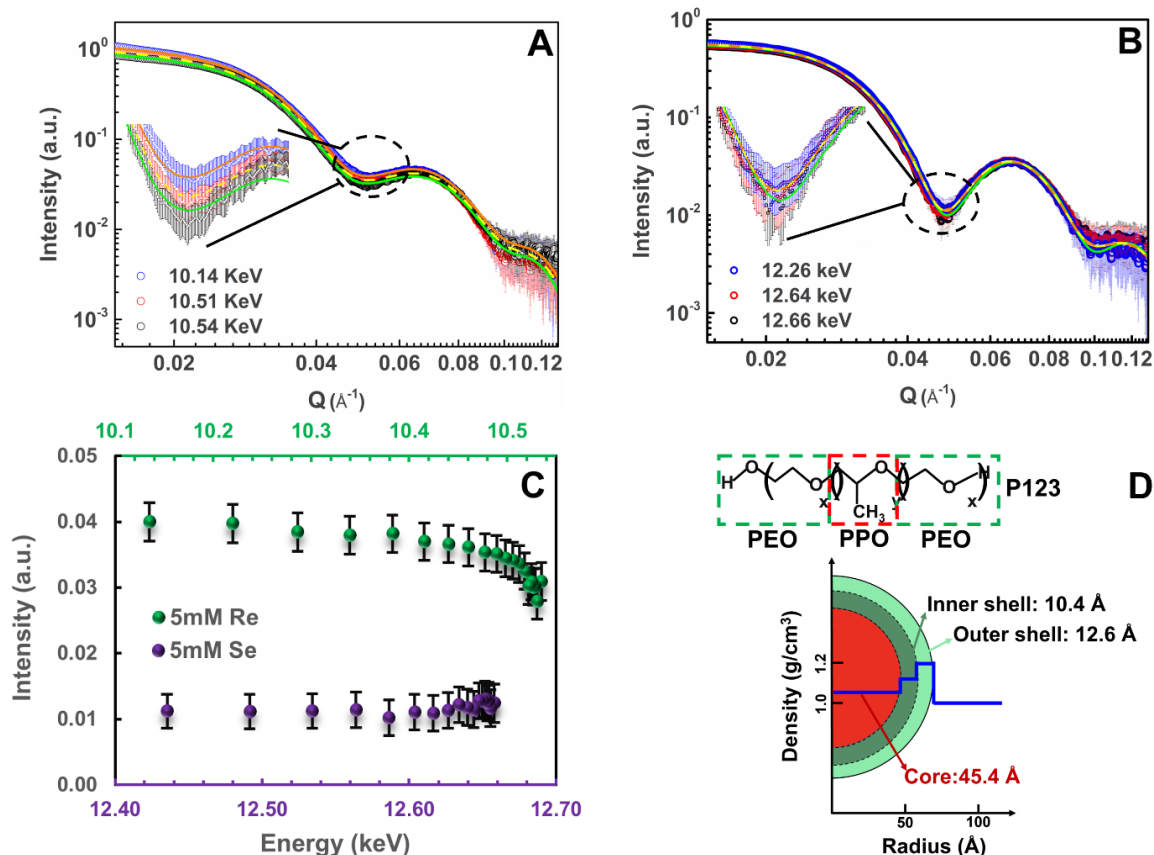
**Figure 1.** ASAXS intensity as a function of wave vector transfer *Q* of an aqueous solution of P123 (5% by weight) containing (A) 5 mM ReO_4^- and (B) 5 mM SeO_4^{2-} at three different energies. (C) X-ray energy dependence of the intensity at Q = 0.05 $Å^{-1}$ for the ReO_4^- and SeO_4^{2-} systems. (D) Real-space multilayered spherical model used to fit ASAXS data. The thickness and density of the core and shells shown by the blue line are measured from a system containing 5 mM ReO_4^-. Other fitting parameters are provided in the SI. Pluronic P123 consists of a block of poly(propylene oxide) (PPO) sandwiched between two blocks of poly(ethylene oxide) (PEO).

Figure 1D illustrates the core-shell model used to fit the ASAXS data in Figures 1A/B. Block copolymer micelles often assemble into core-shell structures.[9] The hydrophobic part of the copolymer will form the core, while the hydrophilic part of the copolymer surrounds the core and

5

forms a shell. Ions distribute within the micelle based on their binding affinity to different regions. The excellent fits to the data shown in Figures 1A/B required a model with two shells and one core, as shown in Figure 1D. Details of ASAXS data analysis can be found in the SI.

Figure 2 illustrates the results of fitting the data in Figure 1, which yields fitting parameters that describe the distribution of ReO_4^- and SeO_4^{2-} within P123 micelles. It is found that ReO_4^- is excluded from the core of the micelle and absorbs with a higher concentration in the outer shell than in the inner shell. Overall, the concentration of ReO_4^- in the micelle increases with the aqueous concentration of ReO_4^-. In comparison, Figures 2A2 and B2 show that SeO_4^{2-} absorbed weakly in the outer shell of the micelle only at the highest concentration of 20 mM. Absorption of SeO_4^{2-} in the inner shell is not observed at any concentration. In addition to anions, we expect absorption of Na^+ cations, though these are not observable in our measurements.


6
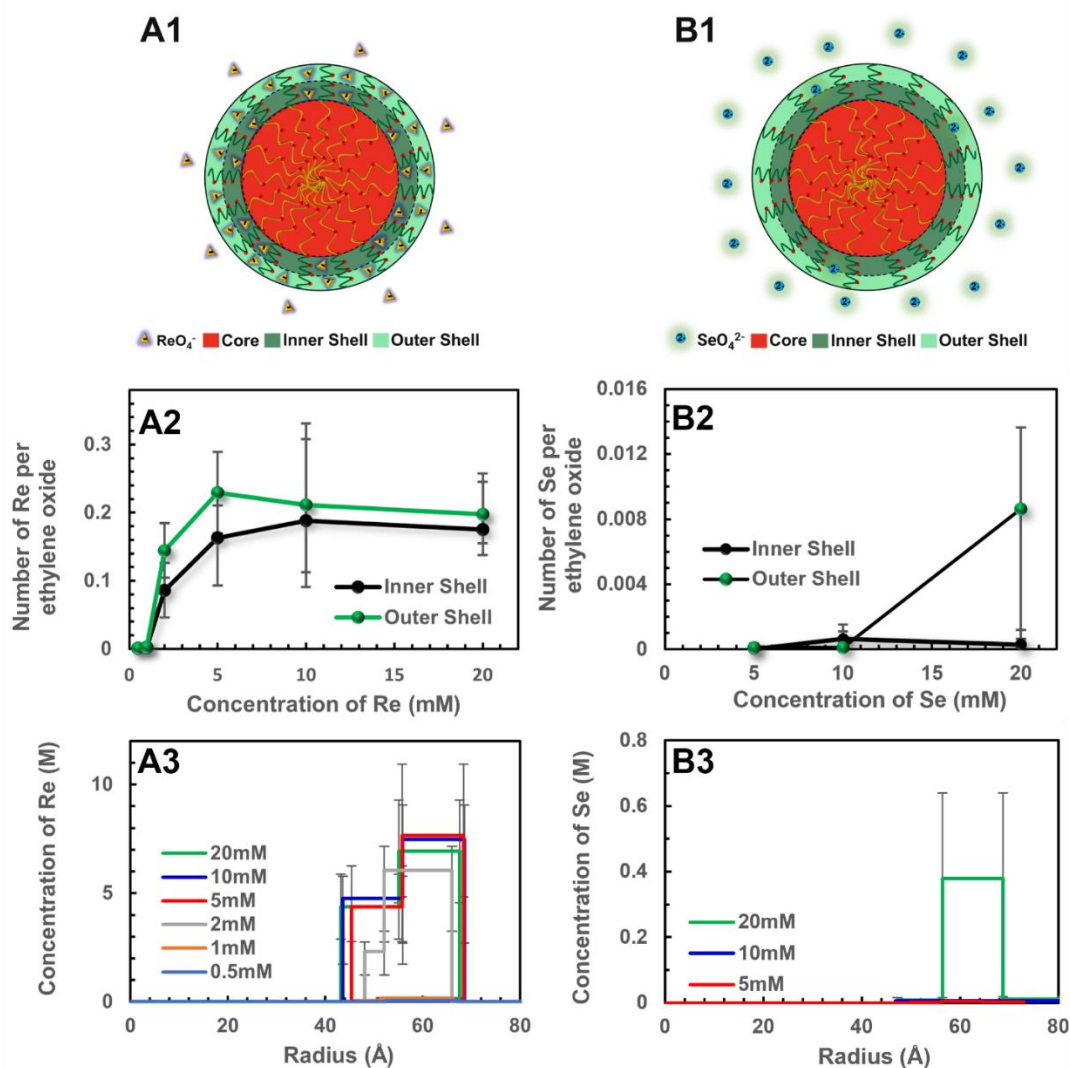
Figure 2. Analysis of ASAXS data. Schematic illustration of the model used to fit the ASAXS data: (A1) ReO_4^-, (B1) SeO_4^{2-}. Fitting parameters as a function of Re or Se concentration in the aqueous solution: (A2) number of ReO_4^- per ethylene oxide, (A3) concentration of Re in the inner and outer shells, (B2) number of SeO_4^{2-} per ethylene oxide, (B3) concentration of Se in the inner and outer shells.

MD simulations of anion distributions in the micelle Classical MD simulations support the anion observations from ASAXS and locate the cations. Figure 3 shows snapshots from simulations of a P123 micelle in the presence of $NaReO_4$ and Na_2SeO_4. Ions ReO_4^- and Na^+ absorb into the region of the PEO block. However, SeO_4^{2-} is mostly excluded from the micelle. These results are consistent with the ASAXS measurements, although the concentrations are not the same (15 wt% of P123 for MD simulations and 5 wt% for experimental samples).

MD analysis of the distribution of polymer blocks and ions in the micelle is shown in Figure 3. Similar to the model used to analyze ASAXS measurements, the micelle can be divided into two shells: an outer shell consisting primarily of hydrophilic PEO which is roughly 25 Å thick and an inner shell of mixed PEO/PPO, which is roughly 15 Å thick and more hydrophobic than the outer shell. Micelles exposed to both types of ions have similar structure and size, except that the PEO outer shell is more dispersed in the presence of SeO_4^{2-}.

When ReO_4^- is present, both shells are enriched in the anion, though the PEO outer shell is more highly enriched. In the presence of SeO_4^{2-}, however, the anion is found exclusively in the PEO outer shell with a net absorption in the micelle that is much lower than for ReO_4^-. Most SeO_4^{2-} ions were located outside the micelle. Sodium ions are found in both shells when either ReO_4^- or SeO_4^{2-} are present, with a preference for the PEO outer shell.

7
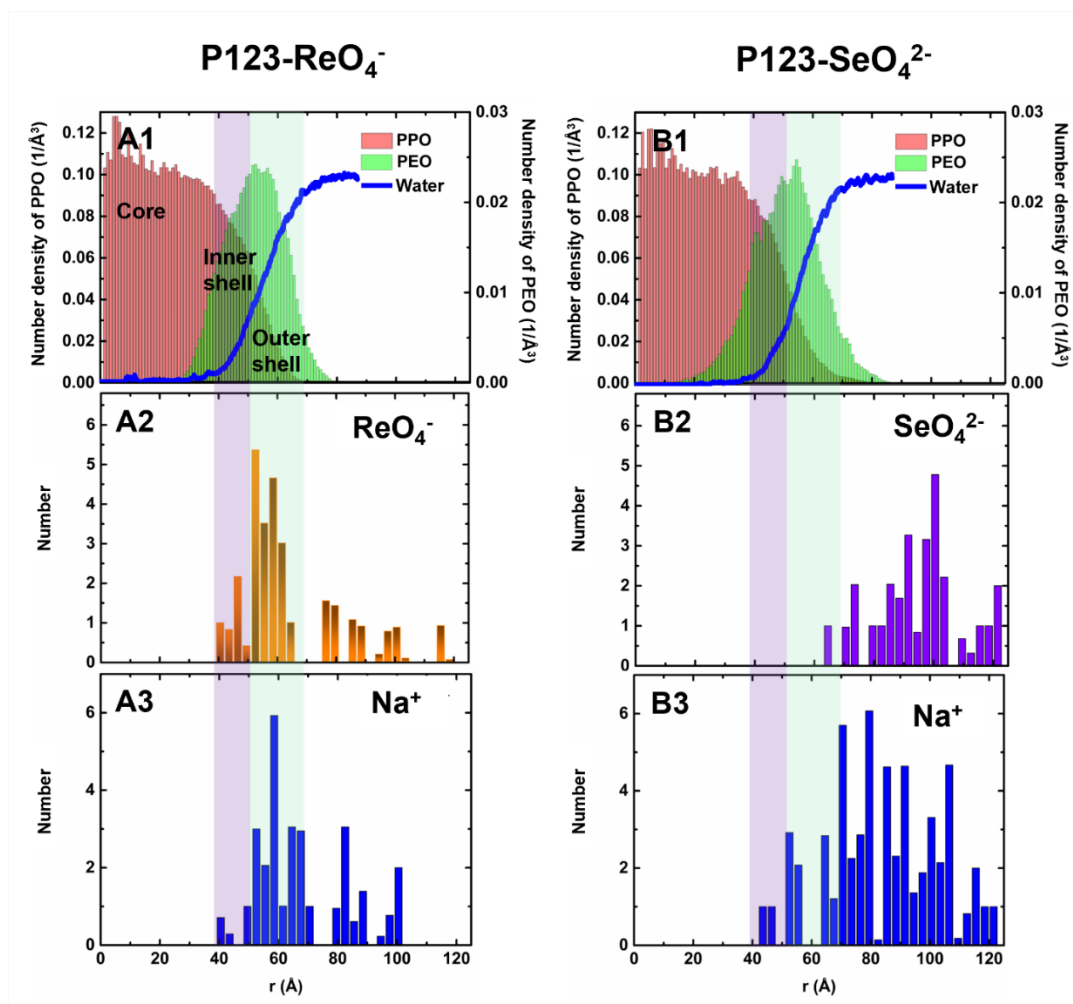
Figure 3. Results of MD simulations with a salt concentration of roughly 10 mM, and 30 Na_2SeO_4 and 30 $NaReO_4$ (see SI for composition and methods). The distribution of ions and polymer blocks (PEO and PPO) in the P123 micelle are shown. Left panels display results for ReO_4^- and right panels for SeO_4^{2-} systems. (A1/B1) number density of PPO/PEO blocks and water across the micelle. (A2/B2) number distribution of anions. (A3/B3) number distribution of Na^+. Vertical colored stripes show estimated regions of a two-shell model. The core and outer shell consist primarily of PPO and PEO, respectively. The inner shell is a nearly equivalent mixture of PPO and PEO.

The distributions of anions in the micelle obtained from MD simulations are qualitatively consistent with the results of the ASAXS measurements. This agreement includes the preferential absorption of ReO_4^- over SeO_4^{2-} in the micelle and the micellar location of ReO_4^- absorption into two shells.
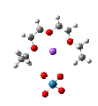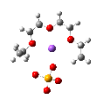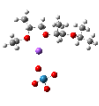
8

**Implications for mechanism of anion-polymer interactions**

These results are likely due to three effects which can influence the binding affinity of anions within a P123 micelle: hydrophobic interactions, confinement effects, and ion dehydration. As discussed below, electrostatic interactions appear to have a minor effect on the distribution of ReO_4^- and SeO_4^{2-} in the micelle despite the different charges of the ions.

1. Electrostatic interactions of ReO_4^- and SeO_4^{2-} with a single polymer chain

Cations, such as Na^+, are known to interact with O atoms on PEO to form a positively charge site.[21,] [40] Anions can then interact electrostatically with P123 via a cation bridge to the oxygen atoms. Density functional theory (DFT) was used to calculate the binding energy of ReO_4^- and SeO_4^{2-} to simplified models of the 2 blocks of P123 in the presence of Na^+ to measure the strength of this interaction. Simplified models consisted of either three monomers of ethylene oxide, (EO)$_3$, or three monomers of propylene oxide, (PO)$_3$. DFT results are summarized in Table 1, which also shows that optimized structures contain a Na^+-bridge between anions and polymer blocks. Notably, the calculations included a water environment surrounding the polymer and anions. Excluding the water environment leads to qualitatively similar conclusions (see SI). Overall, the interactions of both (EO)$_3$ and (PO)$_3$ are stronger with SeO_4^{2-} than with ReO_4^-, which is consistent with the larger charge of SeO_4^{2-}. These model calculations suggest that the electrostatic component of binding of these ions to a single P123 polymer chain is stronger for SeO_4^{2-} than for ReO_4^-.

Table 1. Results from DFT calculations of the interaction energy of different anions with P123 blocks and their optimized structures.

|	Interaction Energy (eV)	Optimized Structure
(EO•Na$^+$)-ReO$_4^-$	-0.13	
(EO•Na$^+$)-SeO$_4^{2-}$	-0.69	
(PO•Na$^+$)-ReO$_4^-$	-0.26	

9
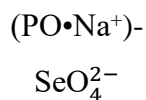
| (PO•Na$^+$)-SeO$_4^{2-}$ | -0.78 | |

2. Crowding and dehydration of ReO_4^- and SeO_4^{2-} within a P123 micelle

ASAXS measurements and MD simulations demonstrate that P123 micelles absorb more ReO_4^- than SeO_4^{2-}, contrary to the stronger binding of SeO_4^{2-} than ReO_4^- to P123 expected from the DFT calculations to short polymer blocks described in the previous section. The microscopic environment within the micelle is different from single chains of P123. As demonstrated, P123 polymer chains self-assemble to form a core-shell structure in water. Polymer chains in the micelle pack closely, enhancing its hydrophobicity and creating a steric barrier for the binding of ions. The hydrophobicity of this core-shell structure decreases from center to surface. The distribution of ions and water across the micelle in Figures 3A1/B1 is consistent with the suggested variation of hydrophobicity within the micelle.

Ion binding in crowded spaces may also require the free energy cost of dehydration to reduce the effective size of the ion. Figure 4 shows snapshots from MD simulations of the interaction of both anions with a P123 micelle. Sodium ions are coordinated with oxygen atoms of the PEO block in both anion systems. ReO_4^- is located between PEO and PPO blocks, and its hydration shell is absent in this crowded space. The SeO_4^{2-} anion remains outside of the micelle. This behavior is consistent with their Gibbs energies of hydration which are much larger for SeO_4^{2-} (-900 kJ/mol) than ReO_4^- (-330 kJ/mol),[38] making it harder for SeO_4^{2-} to dehydrate and enter the micelle.

Although the DFT calculation demonstrated that the binding of anions to a PO block is stronger than to an EO block, the ASAXS and MD results showed that the anions cannot penetrate the micellar core. It appears that the advantage of greater binding by PO has been nullified by the crowded structure of the micellar core.

10
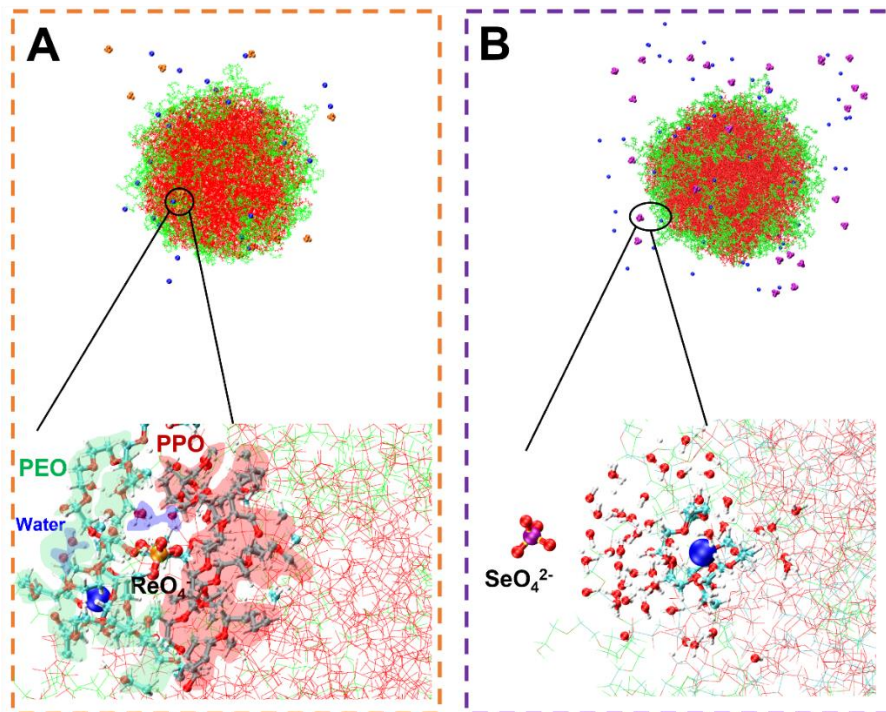
Figure 4. Sections of MD simulation snapshots that illustrate the interaction of anions with a micelle from MD simulations. (A) Interior of micelle showing ReO_4^- ion inside the micelle. (B) Micelle periphery that shows that the SeO_4^{2-} ion does not enter the micelle. Sodium ions are represented by a blue ball; ReO_4^- is represented by yellow and red sticks; SeO_4^{2-} is represented by purple and red sticks; O atoms are red balls. Water surrounding SeO_4^{2-} has been showed transparently for visual clarity. The ReO_4^- dehydrated upon entering the small space between the PPO (red) and PEO (green) blocks of P123.

In conclusion, anion distributions in a Pluronic P123 micelle were obtained from ASAXS measurements and MD simulations. The two ions chosen for study, SeO_4^{2-} and ReO_4^- have different hydration free energies and charges. Both simulations and measurements demonstrated that the strongly hydrated SeO_4^{2-} is mostly excluded from the micelle, while weakly hydrated ReO_4^- absorbs into the outer and inner shells of the micelle along with Na^+ ions. DFT calculations of the electrostatic interactions between the anions and short blocks of PEO and PPO suggested that SeO_4^{2-} should preferentially bind to P123, in contrast to what was observed by ASAXS. Once P123 polymer chains self-assemble to form a micelle, ReO_4^- is preferentially absorbed in the

11

micelle and SeO_4^{2-} is excluded. Spatial confinement of neighboring block copolymer chains within the micelle may prevent fully hydrated ions from entering the micellar environment. The much greater free energy of dehydration of SeO_4^{2-} negates its electrostatic advantage over ReO_4^- in binding to P123. This behavior of anions within micelles is reminiscent of the crowding of macromolecules in cells where physicochemical environments are influenced due to the interactions of confined macromolecules.[41-43] This work highlights the important role of the crowded molecular environment in micelles in regulating anion binding. The fundamental understanding of polymer-anion interactions obtained from the in situ ASAXS measurements facilitate the future design of supramolecular structures in a wide range of applications including ion-channel across the bio-membranes, ion-recognition macromolecular materials, and polymer electrolytes in solid-state batteries.

Acknowledgments

Reference

1. Mai, Y. Y.; Eisenberg, A., Self-assembly of block copolymers. *Chem. Soc. Rev.* **2012,** *41* (18), 5969-5985.

2. Shin, D. W.; Guiver, M. D.; Lee, Y. M., Hydrocarbon-Based Polymer Electrolyte Membranes: Importance of Morphology on Ion Transport and Membrane Stability. *Chem. Rev.* **2017,** *117* (6), 4759-4805.

3. Tu, K. H.; Huang, H.; Lee, S.; Lee, W.; Sun, Z.; Alexander-Katz, A.; Ross, C. A., Machine Learning Predictions of Block Copolymer Self-Assembly. *Adv. Mater.* **2020,** *32* (52), e2005713.

4. Cummins, C.; Lundy, R.; Walsh, J. J.; Ponsinet, V.; Fleury, G.; Morris, M. A., Enabling future nanomanufacturing through block copolymer self-assembly: A review. *Nano Today* **2020,** 35, 100936.

5.   Cui, H.; Chen, Z.; Zhong, S.; Wooley, K. L.; Pochan, D. J., Block copolymer assembly via kinetic control. *Science* **2007,** *317* (5838), 647-50.

6.   Zhang, W., Discrete Block Copolymers for Self-Assembly. *ACS Cent. Sci.* **2020,** *6* (8), 1278-1280.

7.   Jiménez-Ángeles, F.; Kwon, H.-K.; Sadman, K.; Wu, T.; Shull, K. R.; Olvera de la Cruz, M., Self-Assembly of Charge-Containing Copolymers at the Liquid–Liquid Interface. *ACS Cent. Sci.* **2019,** *5* (4), 688-699.

8.   Li, C.; Li, Q.; Kaneti, Y. V.; Hou, D.; Yamauchi, Y.; Mai, Y. Y., Self-assembly of block copolymers towards mesoporous materials for energy storage and conversion systems. *Chem. Soc. Rev.* **2020,** *49* (14), 4681-4736.

9.   Cabral, H.; Miyata, K.; Osada, K.; Kataoka, K., Block Copolymer Micelles in Nanomedicine Applications. *Chem. Rev.* **2018,** *118* (14), 6844-6892.

10.   Butler, S. J.; Parker, D., Anion binding in water at lanthanide centres: from structure and selectivity to signalling and sensing. *Chem. Soc. Rev.* **2013,** *42* (4), 1652-66.

11.   Wei, P.; Yan, X.; Huang, F., Supramolecular polymers constructed by orthogonal self-assembly based on host-guest and metal-ligand interactions. *Chem. Soc. Rev.* **2015,** *44* (3), 815-32.

12.   Pechenkin, M. A.; Möhwald, H.; Volodkin, D. V., pH- and salt-mediated response of layer-by-layer assembled PSS/PAH microcapsules: fusion and polymer exchange. *Soft Matter* **2012,** *8* (33), 8659.

13.   Fong, K. D.; Self, J.; Diederichsen, K. M.; Wood, B. M.; McCloskey, B. D.; Persson, K. A., Ion Transport and the True Transference Number in Nonaqueous Polyelectrolyte Solutions for Lithium Ion Batteries. *ACS Cent. Sci.* **2019,** *5* (7), 1250-1260.

14.   Kudlay, A.; Ermoshkin, A. V.; Olvera de la Cruz, M., Complexation of Oppositely Charged Polyelectrolytes: Effect of Ion Pair Formation. *Macromolecules* **2004,** *37* (24), 9231-9241.

15.   Gregory, K. P.; Wanless, E. J.; Webber, G. B.; Craig, V. S. J.; Page, A. J., The electrostatic origins of specific ion effects: quantifying the Hofmeister series for anions. *Chem. Sci.* **2021,** *12* (45), 15007-15015.

16.   Yoshizawa, M.; Ito-Akita, K.; Ohno, H., Evidence of interaction between anion and polyether in the bulk. *Electrochim. Acta* **2000,** *45* (10), 1617-1621.

17. Lo Nostro, P.; Ninham, B. W., Hofmeister phenomena: an update on ion specificity in biology. *Chem. Rev.* **2012,** *112* (4), 2286-322.

18. Zhang, Y.; Cremer, P. S., Chemistry of Hofmeister Anions and Osmolytes. *Annu. Rev. Phys. Chem.* **2010,** *61* (1), 63-83.

19. Lund, M.; Vácha, R.; Jungwirth, P., Specific Ion Binding to Macromolecules: Effects of Hydrophobicity and Ion Pairing. *Langmuir* **2008,** *24* (7), 3387-3391.

20. Ketkar, P. M.; Shen, K.-H.; Fan, M.; Hall, L. M.; Epps, T. H., Quantifying the Effects of Monomer Segment Distributions on Ion Transport in Tapered Block Polymer Electrolytes. *Macromolecules* **2021,** *54* (16), 7590-7602.

21. Gadjourova, Z.; Andreev, Y. G.; Tunstall, D. P.; Bruce, P. G., Ionic conductivity in crystalline polymer electrolytes. *Nature* **2001,** *412* (6846), 520-523.

22. Jordan, J. H.; Gibb, C. L. D.; Wishard, A.; Pham, T.; Gibb, B. C., Ion-Hydrocarbon and/or Ion-Ion Interactions: Direct and Reverse Hofmeister Effects in a Synthetic Host. *J. Am. Chem. Soc.* **2018,** *140* (11), 4092-4099.

23. Rogers, B. A.; Okur, H. I.; Yan, C.; Yang, T.; Heyda, J.; Cremer, P. S., Weakly hydrated anions bind to polymers but not monomers in aqueous solutions. *Nat. Chem.* **2022,** *14* (1), 40-45.

24. Chandler, D., Interfaces and the driving force of hydrophobic assembly. *Nature* **2005,** *437* (7059), 640-647.

25. O'Brien, J. T.; Prell, J. S.; Bush, M. F.; Williams, E. R., Sulfate Ion Patterns Water at Long Distance. *J. Am. Chem. Soc.* **2010,** *132* (24), 8248-8249.

26. Gurau, M. C.; Lim, S. M.; Castellana, E. T.; Albertorio, F.; Kataoka, S.; Cremer, P. S., On the mechanism of the Hofmeister effect. *J. Am. Chem. Soc.* **2004,** *126* (34), 10522-10523.

27. Rana, B.; Fairhurst, D. J.; Jena, K. C., Investigation of Water Evaporation Process at Air/Water Interface using Hofmeister Ions. *J. Am. Chem. Soc.* **2022.** *144* (39), 17832–17840.

28. Fang, Y.; Furo, I., Weak Anion Binding to Poly(N-isopropylacrylamide) Detected by Electrophoretic NMR. *J. Phys. Chem. B* **2021,** *125* (14), 3710-3716.

29. Hallberg, F.; Furo, I.; Stilbs, P., Ion Pairing in Ethanol/Water Solution Probed by Electrophoretic and Diffusion NMR. *J. Am. Chem. Soc.* **2009,** *131* (39), 13900–13901.

30. Bostrom, M.; Kunz, W.; Ninham, B. W., Hofmeister effects in surface tension of aqueous electrolyte solution. *Langmuir* **2005,** *21* (6), 2619-2623.

31.   dos Santos, A. P.; Diehl, A.; Levin, Y., Surface Tensions, Surface Potentials, and the Hofmeister Series of Electrolyte Solutions. *Langmuir* **2010,** *26* (13), 10778-10783.

32.   Sanada, Y.; Akiba, I.; Sakurai, K.; Shiraishi, K.; Yokoyama, M.; Mylonas, E.; Ohta, N.; Yagi, N.; Shinohara, Y.; Amemiya, Y., Hydrophobic Molecules Infiltrating into the Poly(ethylene glycol) Domain of the Core/Shell Interface of a Polymeric Micelle: Evidence Obtained with Anomalous Small-Angle X-ray Scattering. *J. Am. Chem. Soc.* **2013,** *135* (7), 2574-2582.

33.   Freed, K. F.; Dudowicz, J.; Stukalin, E. B.; Douglas, J. F., General approach to polymer chains confined by interacting boundaries. *J. Chem. Phys.* **2010,** *133* (9), 094901.

34.   Ming, Y. Q.; Zhou, Z. P.; Zhang, S. H.; Wei, Y. Y.; Hao, T. F.; Nie, Y. J., Molecular simulation of crystallization of polymers confined in cylindrical nanodomain. *Polymer* **2020,** *206*, 122818.

35.   Stavrinidou, E.; Leleux, P.; Rajaona, H.; Khodagholy, D.; Rivnay, J.; Lindau, M.; Sanaur, S.; Malliaras, G. G., Direct Measurement of Ion Mobility in a Conducting Polymer. *Adv. Mater.* **2013,** *25* (32), 4488-4493.

36.   Pabit, S. A.; Meisburger, S. P.; Li, L.; Blose, J. M.; Jones, C. D.; Pollack, L., Counting ions around DNA with anomalous small-angle X-ray scattering. *J. Am. Chem. Soc.* **2010,** *132* (46), 16334-6.

37.   Chen, J.; Bera, M. K.; Li, H.; Yang, Y.; Sun, X.; Luo, J.; Baughman, J.; Liu, C.; Yao, X.; Chuang, S. S. C.; Liu, T., Accurate Determination of the Quantity and Spatial Distribution of Counterions around a Spherical Macroion. *Angew. Chem. Int. Ed Engl.* **2021,** *60* (11), 5833-5837.

38.   Marcus, Y., Thermodynamics of solvation of ions. Part 5.—Gibbs free energy of hydration at 298.15 K. *J. Chem. Soc., Faraday Trans.* **1991,** *87* (18), 2995-2999.

39.   Bera, M. K. B., W., XModFit: Xray Modeling and Fitting. *Zenodo* **2022**.

40.   Genier, F. S.; Hosein, I. D., Effect of Coordination Behavior in Polymer Electrolytes for Sodium-Ion Conduction: A Molecular Dynamics Study of Poly(ethylene oxide) and Poly(tetrahydrofuran). *Macromolecules* **2021,** *54* (18), 8553-8562.

41.   Speer, S. L.; Stewart, C. J.; Sapir, L.; Harries, D.; Pielak, G. J., Macromolecular Crowding Is More than Hard-Core Repulsions. *Annu. Rev. Biophys.* **2022,** *51* (1), 267-300.

42.   Estabrook, D. A.; Chapman, J. O.; Yen, S.-T.; Lin, H. H.; Ng, E. T.; Zhu, L.; van de Wouw, H. L.; Campàs, O.; Sletten, E. M., Macromolecular Crowding as an Intracellular Stimulus for Responsive Nanomaterials. *J. Am. Chem. Soc.* **2022,** *144* (37), 16792-16798.

43. Alric, B.; Formosa-Dague, C.; Dague, E.; Holt, L. J.; Delarue, M., Macromolecular crowding limits growth under pressure. *Nat. Phys.* **2022,** *18* (4), 411-416.

TOC
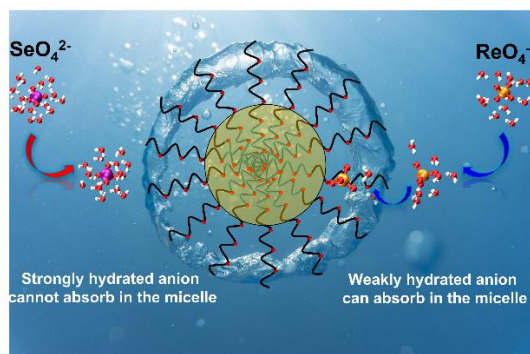
The spatial confinement of crowded neighboring block copolymer chains within the micelle creates a hydrophobic environment where hydrophobic interaction will dominate the interaction of anions with polymers over the electrostatic interaction.